Russian Journal of Organic Chemistry, Vol. 39, No. 5, 2003, pp. 663–671. Translated from Zhurnal Organicheskoi Khimii, Vol. 39, No. 5, 2003, pp. 708–717.

$^{13}C–^{13}C$ Coupling Constants in Structural Studies: XXXIII. Stereochemical Study of the Pyranose Ring

V.A. Danilova and L. B. Krivdin

Angarsk State Technical Academy, ul. Chaikovskogo 60, Angarsk, 665835 Russia
e-mail: krivdin@irk.ru

Received December 29, 2001

Abstract—$^{13}C–^{13}C$ coupling constants for all aldopyranoses of the D-series were calculated in terms of the self-consistent finite perturbation theory. General relations holding in the stereochemical behavior of the $^{13}C–^{13}C$ coupling constants for the pyranose ring were found. The results obtained make it possible to perform conformational analysis and assign configuration of the anomeric center in molecules of carbohydrates and products of their metabolism, containing a pyranose fragment.

Determination of configuration and conformation of the pyranose ring in carbohydrates, nucleic acids, nucleotides, nucleosides, purine bases, proteins, co-enzymes, and products of their metabolism is very important for studying and predicting their biological activity [1]. NMR spectroscopy is widely used to ascertain the configuration of anomeric center and for conformational analysis of biological molecules containing carbohydrate fragments [2]. Here, relevant parameters are spin–spin coupling constants for those carbon nuclei which exhibit pronounced stereochemical effects, depending on the arrangement of neighboring atoms and groups and conformation of the molecule [3, 4].

The available experimental data on $^{13}C–^{13}C$ coupling constants in carbohydrates [5, 6] suggest that these quantities are sensitive to stereochemical effects determined by molecular conformation and configuration of the anomeric center. Specific interest in $^{13}C–^{13}C$ coupling constants for carbohydrates arises from wide application in biochemical studies of carbohydrates and their derivatives selectively enriched with the ^{13}C isotope [2]. Experimental measurement of $^{13}C–^{13}C$ coupling constants in such systems is a common routine: they can be determined directly from a standard ^{13}C NMR spectrum with broad-band decoupling from protons. In the present work we performed theoretical calculations of $^{13}C–^{13}C$ coupling constants for pyranose ring with the goal of studying stereochemical relations holding therein and elucidating possible ways of their use in stereochemical analysis of biomolecules having a pyranose ring.

It is known that cyclic monosaccharides give rise to two anomeric forms (or configurations). A carbohydrate molecule is refferred to as α-anomer if the configuration of the anomeric center (at the semiacetal hydroxy group, C^1) coincides with that of the asymmetric carbon atom which determines its pertinence to the D- or L-series (C^5). In addition, each anomer can exist as an equilibrium mixture of normal (C1) and alternative (1C) *chair* conformers, as shown below using glucose as an example:

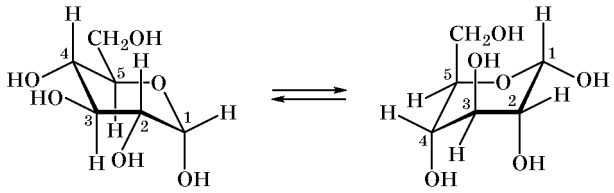

α-D-Glucose C1 ⇌ α-D-Glucose 1C

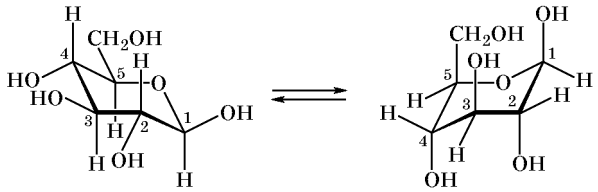

β-D-Glucose C1 ⇌ β-D-Glucose 1C

Assignment of configuration of the anomeric center in carbohydrates, their metabolites, and other biological molecules having a pyranose fragment is not always unambiguous, and conformational analysis of these species by conventional methods is not always

possible. In order to reveal new potentialities in stereochemical analysis of carbohydrates, we calculated direct $^{13}C–^{13}C$ coupling constants for the anomeric carbon atom in α- and β-anomers of all four possible aldopentopyranoses and eight aldohexopyranoses of the D-series. The calculations were performed in terms of the self-consistent finite perturbation theory (SCPT) in the INDO approximation. Our interest in the $^1J_{1,2}$ coupling constant originates from the fact that just this constant is most sensitive to configuration and conformation of the pyranose ring [3, 5, 6].

Semiempirical calculations of $^{13}C–^{13}C$ coupling constants in organic molecules are based on the use of empirical parameters, specifically of those setting *s*-electron density on carbon atoms and radii of their *p* orbitals. Such calculations require a proper choice of the procedure for optimization of geometric parameters. It is especially important in the case of carbohydrates for which rotation of hydroxy groups about the C−O bonds should be taken into account [7]. We performed a comparative analysis of traditional NDDO semiempirical methods for geometry optimization (MNDO, AM1, PM3), as well as of nonempirical methods, including those based on the restricted Hartree–Fock theory for closed shells (RHF) and the density functional theory (DFT) involving the most popular Becke three-parameter hybrid functional [8] in combination with the Lee–Yang–Parr functional (B3LYP) [9]. Geometry optimization in terms of the DFT–B3LYP method was performed with the use of the Pople standard polarization basis set 6-31G** [10] (which includes polarization *p*-functions on hydrogen atoms and polarization *d*-functions on carbon and oxygen atoms) and the Dunning standard correlation-consistent polarization basis set cc-pVDZ [11] which employs analogous sets of polarization functions but with different contraction coefficients. The results showed that both semiemperical and nonempirical geometry optimization methods overestimate the $C^1–C^2$ bond length on the average by 0.02 Å relative to the experimental X-ray diffraction data (this is explained by tight molecular packing in crystal). The bond angles $O^5C^1C^2$, HC^1C^2, $O^2C^2C^1$, and HC^2C^1 are reproduced well by all methods with an accuracy of 1–2°, while the bond angle $O^1C^1C^2$ at the anomeric center is always overestimated by 4–8° relative to the experimental value 107.8°. By contrats, the endocyclic bond angle $C^3C^2C^1$ is always underestimated by 4–6° (experimental value 113.2°). The above differences between the calculated and experimental bond angles can also be attributed to distortion of the structure of β-D-glucose in the crystalline lattice. The dihedral angle HC^1C^2H is reproduced by the MNDO and AM1 methods with an accuracy of 1°, whereas the PM3 procedure gives considerably poorer results. On the other hand, DFT–B3LYP nonempirical calculations surprisingly overestimate the HC^1C^2H angle (on the average, by 4°), while the classical RHF/6-31G** procedure gives a value of 177.1° which exceeds by 2° the experimental angle (175.2°). On the whole, the B3LYP method with both 6-31G** and cc-pVDZ basis sets is characterized by the minimal average relative error (1.7–1.9%), i.e., it reproduces best the experimental geometry. The maximal average relative error (3.4%) was found for the PM3 method. Semiempirical MNDO and AM1 methods, as well as nonempirical RHF procedure, are characterized by an average relative error of 2.1–2.6%.

As concerns $^1J_{1,2}$ values calculated with the use of geometric parameters optimized by different methods, the AM1 procedure ensured the best agreement with the experimental value: $^1J_{1,2}$ = 46.2 Hz against 46.0 Hz [12]. On the whole, semiempirical geometry optimization methods overestimate $^1J_{1,2}$; the largest $^1J_{1,2}$ value (49.2 Hz) was obtained by the MNDO method. By contrast, nonempirical methods give lower $^1J_{1,2}$ values than that found experimentally, the lowest value being obtained with B3LYP/6-31G** geometry optimization (41.3 Hz).

Thus, comparison of the optimized geometric parameters of β-D-glucose C1 with the X-ray diffraction data does not allow us to prefer nonempirical methods over semiempirical, though nonempirical RHF and DFT-B3LYP calculations with the 6-31G** basis set give somewhat better results. Among the nonempirical methods, B3LYP reproduces the experimental geometry most accurately with the use of the Pople standard polarization basis set 6-31G**, while the Dunning standard correlation-consistent polarization basis set cc-pVDZ gives slightly worse results. Similar results were obtained by RHF calculations with the same basis sets.

Among the semiempirical methods, best reproduction of the experimental geometry was achieved with MNDO and AM1 which are traditionally used for geometry optimization of organic compounds. However, MNDO optimization of geometric parameters is inferior to AM1 in the calculation of the coupling constants. The PM3 method gives the maximal average relative error (3.4%) in the reproduction of experimental geometry; in addition, it considerably overestimates the coupling constant.

Undoubtedly, while selecting a procedure for optimization of geometric parameters we were interested

in reliable reproduction of the experimental geometry, but the problem of reproduction of experimental ^{13}C–^{13}C coupling constants was nevertheless more important. In addition, taking into account a great deal of calculations, we also aimed at shortening the computation time (for example, geometry optimization of only one form of β-D-glucose C1 by the B3LYP/cc-pVDZ method takes more than 8 days). For this purpose, we examined $^1J_{1,2}$ values for normal and alternative conformations of both anomers of mannose, calculated by the SCPT INDO method with geometric parameters optimized by different procedures, and compared them with the available experimental data. Using semiempirical MNDO and PM3 methods for geometry optimization, we obtained clearly overestimated coupling constants $^1J_{1,2}$. The results obtained with the AM1 method were comparable with those derived from nonempirical RHF and DFT–B3LYP calculations. The best agreement with the experimental coupling constant $^1J_{1,2}$ for α-D-mannose C1 (46.7 Hz) was observed with the use of AM1 geometry optimization (46.9 Hz), and for β-D-mannose C1 (experimental value 42.7 Hz), with the RHF/cc-pVDZ method. In the latter case, the calculated $^1J_{1,2}$ value was exactly the same as experimental.

It should be noted that the C^1-C^2 bond in all the examined forms of mannose, optimized by the semiempirical methods, is considerably longer than the C^1-C^2 bond optimized by the nonempirical methods and that the MNDO method gives unreasonably overestimated values. Similar results were obtained for bond angles. We can conclude that the use of MNDO and PM3 is clearly inappropriate, while the results of AM1 calculations approach those obtained by the nonempirical RHF and DFT–B3LYP methods. It should be kept in mind that in all cases the ^{13}C–^{13}C coupling constants were calculated on a semiempirical level (SCPT INDO) [13]. Taking into account the results of comparative analysis of different methods for optimization of geometric parameters (with respect to reproduction of both experimental geometry and experimental ^{13}C–^{13}C coupling constants) and the problem of saving computation time, in all subsequent calculations of $^1J_{1,2}$ for the series of pento- and hexopyranoses **I**–**XXIV** we used geometric parameters optimized by the semiempirical AM1 method.

Table 1 contains the calculated coupling constants $^1J_{1,2}$ for four pentopyranoses: ribose, arabinose, lyxose, and xylose; the corresponding values for eight hexopyranoses: allose, altrose, glucose, mannose, gulose, idose, galactose, and talose are given in Table 2. Depending on the steric structure of the pyranose ring, the range of variation of the calculated $^1J_{1,2}$ values exceeds 5 Hz. A good agreement between the calculated and available experimental data is observed. It should be noted that any experimentally measured coupling constant refers to an equilibrium mixture of the normal and alternative conformers. Therefore, comparison of the calculated and experimental data is justified only when one conformer is known to predominate. For example, β-D-lyxose exists mainly as C1 conformer (87%) [5, 12], and Table 1 contains the experimental $^1J_{1,2}$ value (in parentheses) only for β-D-lyxose C1 (**VIIIa**). α-D-Lyxose consists of 38% of 1C conformer and 62% of C1 conformer [5, 12], i.e., the fractions of its normal and alternative conformers are comparable; therefore, the experimental coupling constant for the α-anomer of lyxose (**VIIa**, **VIIb**) was given twice (Table 1). The same applies to α-D-ribose (**IIIa**, **IIIb**), α-D-altrose (**XIa**, **XIb**), and α-D-idose (**XIXa**, **XIXb**) [12]. Nevertheless, the difference between the calculated and experimental ^{13}C–^{13}C coupling constants as a rule does not exceed 1–2 Hz, which is comparable with the experimental error in their determination from survey ^{13}C NMR spectra recorded with broad-band decoupling from protons from samples selectively enriched in ^{13}C isotope.

In the framework of the Ramsey fundamental nonrelativistic perturbation theory of spin–spin interaction [14], the total coupling constant value includes three different constituents originating from three physically indistinguishable mechanisms of nuclear magnetic spin interaction through bond electrons (indirect spin–spin interaction): Fermi-contact (FC), which is a contact interaction between nuclear and electron spins directly on the nucleus surface; spin–dipole (SD), which is a dipole interaction between spatially separated (in contrast to the contact interaction) nuclear and electron spins; and spin–orbital (SO), which is an interaction of nuclear spins with the orbital angular moments of electrons (here, we do not consider division of spin–orbital interaction into diamagnetic and paramagnetic constituents). Then, the total coupling constant may be represented as the sum of the above three contributions:

$$J = J_{FC} + J_{SD} + J_{SO}. \quad (1)$$

These contributions together with the total $^1J_{1,2}$ values for pyranoses **I**–**XXIV** are given in Tables 1 and 2. It is seen that in all cases the Fermi-contact contribution prevails. The negative spin–orbital contribution varies within a very narrow range from –2.3 to –2.1 Hz, whereas the positive spin–dipole contribution is the same for all the examined compounds and

Table 1. C^1–C^2 coupling constants (Hz) in pentopyranoses, calculated by the SCPT INDO method

Compound	Orientation of the OH group on C^1 and C^2	J_{SO}	J_{SD}	J_{FC}	$^1J_{1,2}$[a]
D-Arabinose					
α-D-Ara-C1 (**Ia**)	*aa*	–2.2	1.4	46.1	45.3
α-D-Ara-1C (**Ib**)	*ee*	–2.1	1.4	47.1	46.4 (45.7)
β-D-Ara-C1 (**IIa**)	*ea*	–2.2	1.4	46.5	45.7
β-D-Ara-1C (**IIb**)	*ae*	–2.1	1.4	46.8	46.1 (45.7)
D-Ribose					
α-D-Rib-C1 (**IIIa**)	*ae*	–2.1	1.4	45.5	44.8 (43.2)
α-D-Rib-1C (**IIIb**)	*ea*	–2.2	1.4	45.7	44.9 (43.2)
β-D-Rib-C1 (**IVa**)	*ee*	–2.1	1.4	48.8	48.1 (47.0)
β-D-Rib-1C (**IVb**)	*aa*	–2.1	1.4	48.2	47.5
D-Xylose					
α-D-Xyl-C1 (**Va**)	*ae*	–2.1	1.4	46.7	46.0 (46.1)
α-D-Xyl-1C (**Vb**)	*ea*	–2.3	1.4	46.5	45.7
β-D-Xyl-C1 (**VIa**)	*ee*	–2.1	1.4	47.1	46.4 (45.9)
β-D-Xyl-1C (**VIb**)	*aa*	–2.2	1.4	49.4	48.6
D-Lyxose					
α-D-Lyx-C1 (**VIIa**)	*aa*	–2.2	1.4	47.8	47.1 (47.1)
α-D-Lyx-1C (**VIIb**)	*ee*	–2.1	1.4	48.4	47.7 (47.1)
β-D-Lyx-C1 (**VIIIa**)	*ea*	–2.2	1.4	45.3	44.5 (43.2)
β-D-Lyx-1C (**VIIIb**)	*ae*	–2.1	1.4	48.4	47.7

[a] In parentheses are given the experimental coupling constants from review [3] for predominant conformers or comformers present in comparable amounts.

is equal to 1.4 Hz. The overall contribution from the noncontact interactions with opposite signs is negligible, and it almost does not depend on the conformation or configuration of the pyranose ring.

Thus, just the Fermi-contact contribution makes the ^{13}C–^{13}C coupling constant sensitive to stereochemical effects in the pyranose ring. This conclusion is important, for nonempirical calculations of ^{13}C–^{13}C coupling constant in carbohydrates, which normally require tremendous computer power, could be limited to calculation of only Fermi-contact interaction. It is known that calculation of the latter is by an order of magnitude less expensive than analogous calculation of the spin–dipole contribution. Such calculations of carbohydrates in terms of the density functional theory (DFT–B3LYP) have recently been performed for the first time [7, 15].

Detailed analysis of the variation of $^1J_{1,2}$ values (Tables 1, 2) allowed us to reveal the following stereochemical relations:

(1) Normal conformations of pento- and hexopyranoses with axial orientation of the hydroxy group on C^2 are characterized by greater $^1J_{1,2}$ values for the α-anomers than for the β-anomers by about 3 Hz. In the α-anomers, the hydroxy groups on C^1 and C^2 are axial, i.e., they are arranged *trans* with respect to each other. In the β-anomers, the hydroxy group on C^1 is equatorial. This relation is clearly observed for normal conformers of lyxose (**VIIa** and **VIIIa**), mannose (**XVa** and **XVIa**), idose (**XIXa** and **XXa**), and talose (**XXIIIa** and **XXIVa**). The difference in the coupling constants (~3 Hz) is quite sufficient for unambiguous assignment of configuration of the anomeric center;

(2) Contrastingly, in normal conformers of pento- and hexopyranoses with equatorial orientation of the hydroxy group on C^2, the coupling constant $^1J_{1,2}$ is greater for the β-anomers in which the hydroxy groups on C^1 and C^2 both are equatorial; i.e., they appear *gauche* with respect to each other. This relation is expressed very weakly for normal conformers of xylose (**Va** and **VIa**), glucose (**XIIIa** and **XIVa**), and galactose (**XXIa** and **XXIIa**), for which the difference in the coupling constants is less than 1 Hz, but is clearly seen for normal conformers of ribose (**IIIa** and

Table 2. C^1–C^2 coupling constants (Hz) in hexopyranoses, calculated by the SCPT INDO method

Compound	Orientation of the OH group on C^1 and C^2	J_{SO}	J_{SD}	J_{FC}	$^1J_{1,2}$[a]
D-Allose					
α-D-All-C1 (**IXa**)	*ae*	–2.1	1.4	45.5	44.8 (45.4)
α-D-All-1C (**IXb**)	*ea*	–2.3	1.4	44.2	43.4
β-D-All-C1 (**Xa**)	*ee*	–2.1	1.4	48.6	47.9 (47.3)
β-D-All-1C (**Xb**)	*aa*	–2.2	1.4	47.0	46.2
D-Altrose					
α-D-Alt-C1 (**XIa**)	*aa*	–2.2	1.4	46.0	45.2 (46.2)
α-D-Alt-1C (**XIb**)	*ee*	–2.1	1.4	46.5	45.9 (46.2)
β-D-Alt-C1 (**XIIa**)	*ea*	–2.3	1.4	46.3	45.5 (43.9)
β-D-Alt-1C (**XIIb**)	*ae*	–2.1	1.4	46.5	45.8
D-Glucose					
α-D-Glc-C1 (**XIIIa**)	*ae*	–2.1	1.4	46.5	45.8 (46.2)
α-D-Glc-1C (**XIIIb**)	*ea*	–2.3	1.4	45.2	44.4
β-D-Glc-C1 (**XIVa**)	*ee*	–2.1	1.4	46.8	46.2 (46.0)
β-D-Glc-1C (**XIVb**)	*aa*	–2.2	1.4	48.3	47.5
D-Mannose					
α-D-Man-C1 (**XVa**)	*aa*	–2.2	1.4	47.6	46.9 (46.7)
α-D-Man-1C (**XVb**)	*ee*	–2.1	1.4	47.9	47.2
β-D-Man-C1 (**XVIa**)	*ea*	–2.2	1.4	45.0	44.2 (42.7)
β-D-Man-1C (**XVIb**)	*ae*	–2.2	1.4	47.4	46.6
D-Gulose					
α-D-Gul-C1 (**XVIIa**)	*ae*	–2.1	1.4	48.4	47.7 (45.9)
α-D-Gul-1C (**XVIIb**)	*ea*	–2.3	1.4	44.7	43.8
β-D-Gul-C1 (**XVIIIa**)	*ee*	–2.1	1.4	48.4	47.6 (47.7)
β-D-Gul-1C (**XVIIIb**)	*aa*	–2.2	1.4	47.3	46.6
D-Idose					
α-D-Ido-C1 (**XIXa**)	*aa*	–2.2	1.4	49.5	48.7 (46.2)
α-D-Ido-1C (**XIXb**)	*ee*	–2.1	1.4	46.5	45.8 (46.2)
β-D-Ido-C1 (**XXa**)	*ea*	–2.3	1.4	46.7	45.9 (43.8)
β-D-Ido-1C (**XXb**)	*ae*	–2.1	1.4	46.3	45.6
D-Galactose					
α-D-Gal-C1 (**XXIa**)	*ae*	–2.1	1.4	46.7	46.0 (46.0)
α-D-Gal-1C (**XXIb**)	*ea*	–2.3	1.4	45.8	44.9
β-D-Gal-C1 (**XXIIa**)	*ee*	–2.1	1.4	46.8	46.1 (45.9)
β-D-Gal-1C (**XXIIb**)	*aa*	–2.2	1.4	49.0	48.2
D-Talose					
α-D-Tal-C1 (**XXIIIa**)	*aa*	–2.2	1.4	48.3	47.5 (46.5)
α-D-Tal-1C (**XXIIIb**)	*ee*	–2.1	1.4	48.2	47.5
β-D-Tal-C1 (**XXIVa**)	*ea*	–2.3	1.4	45.7	44.8 (42.3)
β-D-Tal-1C (**XXIVb**)	*ae*	–2.2	1.4	45.5	44.7

[a] In parentheses are given the experimental coupling constants from review [3] for predominant conformers or comformers present in comparable amounts.

IVa) and allose (**IXa** and **Xa**). In the latter cases, the difference in the coupling constants exceeds 3 Hz;

(3) The $^1J_{1,2}$ values for alternative conformations of pento- and hexopyranoses with axial hydroxy group on C^2 are on the average by 3 Hz greater for the β-anomers with axial hydroxy group on C^1 than for the α-anomers in which the hydroxy group on C^1 is equatorial. This pattern is observed for alternative conformers of ribose (**IIIb** and **IVb**), xylose (**Vb** and **VIb**), allose (**IXb** and **Xb**), glucose (**XIIIb** and **XIVb**), gulose (**XVIIIb** and **XVIIIb**) and galactose (**XXIb** and **XXIIb**);

(4) By contrast, alternative conformations of pento- and hexopyranoses with equatorial hydroxy group on C^2 are characterized by greater $^1J_{1,2}$ values for the α-anomers in which the hydroxy group on C^1 is also equatorial, so that it is arranged *gauche* with respect to 2-OH. This tendency is seen most clearly for alternative conformers of talose (**XXIIIb** and **XXIVb**), and it is much weaker for mannose (**XXVb** and **XXVIb**), arabinose (**Ib** and **IIb**), and idose (**XIXb** and **XXb**);

(5) For the α-anomers of pyranoses with different orientations of the hydroxy groups on C^1 and C^2, the $^1J_{1,2}$ values for normal conformers C1 (with axial hydroxy group on C^1 and equatorial hydroxy group on C^2) are greater by 1–4 Hz than the corresponding values for the alternative conformer (with equatorial hydroxy group on C^1 and axial hydroxy group on C^2). This relation is typical of the α-anomers of allose (**IXa** and **IXb**), glucose (**XIIIa** and **XIIIb**), gulose (**XVIIa** and **XVIIb**), and galactose (**XXIa** and **XXIb**);

(6) On the other hand, the β-anomers of pyranoses with different orientations of the hydroxy groups on C^1 and C^2 are characterized by smaller $^1J_{1,2}$ values (by 2–3 Hz) for the normal conformers where the anomeric hydroxy group is equatorial and the hydroxy group on C^2 is axial, as compared to the alternative conformer (with axial hydroxy group on C^1 and equatorial hydroxy group on C^2). This pattern is observed, e.g., for β-D-lyxose (**VIIIa** and **VIIIb**) and β-D-mannose (**XVIa** and **XVIb**).

The above data demonstrate a pronounced stereospecificity of the $^{13}C–^{13}C$ coupling constants in carbohydrates with respect to (1) orientation of the anomeric hydroxy group in the conformationally homogeneous anomers, e.g., in the normal conformers of α- and β-anomers of lyxose (**VIIa** and **VIIIa**) and mannose (**XVa** and **XVIa**), and (2) different conformations of the same anomer, e.g., as in α-D-gulose C1 and α-D-gulose 1C (**XVIIa** and **XVIIb**) and in β-D-galactose C1 and β-D-galactose 1C (**XXIIa** and **XXIIb**). The available experimental data (which were excellently reproduced by our calculations) confirm mainly the first two of the above six relations, which make it possible to assign the configuration of anomeric center in the normal conformation of pyranoses. On the other hand, the remaining relations allow us to determine the configuration of anomeric center in pyranoses existing in the alternative conformation, as well as to perform conformational analysis of biological molecules having a pyranose fragment; these relations were established by us for the first time.

The above six relations may be regarded as a practical guide to assignment of the configuration of anomeric center and conformational analysis of the pyranose ring in carbohydrates. They can be reduced to three simple and more general rules which associate the $^{13}C–^{13}C$ coupling constant with orientation of the hydroxy groups on C^1 and C^2 of the pyranose ring:

(1) Carbohydrates in which the hydroxy groups on C^1 and C^2 both are axial (*aa*) are characterized by considerably larger coupling constant $^1J_{1,2}$ than those (the other anomer or conformer) having equatorial anomeric hydroxy group and axial hydroxy group on C^2 (*ea*);

(2) The coupling constant $^1J_{1,2}$ for a carbohydrate with axial anomeric hydroxy group and equatorial hydroxy group on C^2 (*ae*) is larger than that for its other anomer or conformer with equatorial hydroxy group on C^1 and axial hydroxy group on C^2 (*ea*);

(3) The coupling constant $^1J_{1,2}$ for a carbohydrate with equatorial hydroxy groups on C^1 and C^2 (*ee*) is as a rule larger than that for its other anomer or conformer with axial anomeric hydroxy group and equatorial hydroxy group on C^2 (*ae*).

Taking into account the importance of our results for stereochemical analysis of carbohydrates, we tried to interpret the above relations in terms of the CLOPPA approach [16] which considers contributions from particular localized molecular orbitals (LMO) to the total $^{13}C–^{13}C$ coupling constant in the INDO approximation. The total coupling constants calculated by the CLOPPA and SCPT methods in the INDO approximation are identical.

In terms of the CLOPPA approach, which is based on the polarization propagator theory [17], the coupling constant $^1J_{1,2}$ is considered to consist of a large number of elementary contributions J_{ia}, J_{jb} arising from two-species excitation with participation of two occupied (*i*, *j*) and two vacant (*a*, *b*) LMOs. The latter can be related to lone electron pairs on the oxygen atom and chemical bonds of interest in the pyranose fragment according to the MO localization:

$$^{1}J_{1,2} = \sum_{ia,jb} J_{ia,jb}; \quad (2)$$

$$\hat{J}_{ia,jb} = \Omega\, \hat{J}_{ia,1}\, {}^{s}P_{ia,jb}\, \hat{J}_{jb,2}. \quad (3)$$

Here, ${}^{s}P_{ia,jb}$ is the polarization propagator matrix which is affected by the perturbation operators $\hat{J}_{ia,1}$ and $\hat{J}_{jb,2}$ corresponding to the above listed spin–spin interaction mechanisms (here, only the Fermi-contact interaction was taken into account, for the contributions from noncontact interactions were negligible), and Ω is a numerical constant.

In order to determine factors responsible for the observed stereochemical effects, we selected a set of pyranoses for which these effects are pronounced most strongly. On the one hand, the set included pyranose anomers for which the difference in $^{1}J_{1,2}$ is related to different configurations of the anomeric center (the first four pairs); on the other hand, these were different conformers of the same anomer, for which the difference in $^{1}J_{1,2}$ is related to different conformations of the pyranose ring (the latter three pairs).

Table 3 gives the most interesting LMO contributions to $^{1}J_{1,2}$, calculated by the known Engelmann procedure for localization of initial molecular orbitals [17]. This procedure involves representation of LMO as a linear combination of canonical MOs in such a way that their projection onto the selected AO basis be maximal. Thus, one localization step gives one or several LMOs with maximal projections onto the selected basis of atomic orbitals which describe a particular molecular fragment, chemical bond, or lone electron pair on a heteroatom. At each next localization step, the number of nonlocalized MOs is reduced at the expense of LMOs obtained at preceding steps, which are not involved in localization at the given step.

However, unlike the multistep Engelmann procedure, in the present work each lone electron pair (as one bonding MO) and each chemical bond (as one occupied and one antibonding MO) were localized separately by one-step procedure for each molecular fragment of each form of carbohydrate. We believe that such approach is more correct though considerably more laborious.

The data in Table 3 show that the most significant contribution to $^{1}J_{1,2}$ is that from the C^1-C^2 bond. It even exceeds the calculated total values on the average by 15%. Next follow the contributions of the C^1-H and C^2-H bonds (2.2, and 5.4%, respectively), while the contributions of the C^1-O^1 and C^2-O^2 bonds turned out to be insignificant (less than 1%).

The overall contributions from lone electrone pairs of two oxygen atoms O^1 and O^2 as a rule do not exceed 1 Hz (less than 2% of the total value), whereas the contributions from both O–H bonds (at C^1 and C^2) are equal to zero. This result was quite surprising.

Table 3. Contributions of LMOs to the coupling constant $^{1}J_{1,2}$, calculated by the CLOPPA INDO method

Compound	Configuration	Contributions of LMOs to $^{1}J_{1,2}$, Hz									$^{1}J_{1,2}$,[a] Hz
		O^1[b]	O^1–H	C^1–H	C^1–O^1	O^2[b]	O^2–H	C^2–H	C^2–O^2	C^1–C^2	
α-D-Lyx-C1 (**VIIa**)	*aa*	0.7	0.0	1.6	0.3	–0.1	0.0	2.4	0.0	53.8	47.1 (47.1)
β-D-Lyx-C1 (**VIIIa**)	*ea*	0.9	0.0	–0.2	0.1	0.0	0.0	2.5	0.0	51.8	44.5 (43.2)
α-D-Man-C1 (**XVa**)	*aa*	0.6	0.0	1.6	0.3	0.0	0.0	2.5	0.0	53.4	46.9 (46.7)
β-D-Man-C1 (**XVIa**)	*ea*	1.0	0.0	–0.3	0.1	0.0	0.0	2.5	0.0	51.2	44.2 (42.7)
α-D-Xyl-1C (**Vb**)	*ea*	0.7	0.0	0.0	0.1	0.5	0.0	2.0	0.0	52.8	45.7 (46.1)
β-D-Xyl-1C (**VIb**)	*aa*	0.6	0.0	1.8	0.3	0.5	0.0	2.1	0.1	55.6	48.6 (45.9)
α-D-All-1C (**IXb**)	*ea*	0.9	0.0	–0.3	0.1	0.3	0.0	2.5	0.0	50.2	43.4 (45.4)
β-D-All-1C (**Xb**)	*aa*	0.5	0.0	1.8	0.3	–0.7	0.0	2.5	0.0	52.4	46.2 (47.3)
α-D-Gul-C1 (**XVIIa**)	*ae*	0.4	0.0	1.5	0.2	0.3	0.0	2.2	0.0	54.5	47.7 (45.9)
α-D-Gul-1C (**XVIIb**)	*ea*	0.9	0.0	–0.2	0.1	0.0	0.0	2.5	0.0	50.8	43.8 (45.9)
α-D-Ido-C1 (**XIXa**)	*aa*	0.3	0.0	1.8	0.2	0.6	0.0	2.1	0.1	55.6	48.7 (46.2)
α-D-Ido-1C (**XIXb**)	*ee*	1.0	0.0	0.5	0.1	0.5	0.0	3.3	0.0	52.6	45.8 (46.2)
β-D-Gal-C1 (**XXIIa**)	*ee*	0.8	0.0	0.7	0.1	0.9	0.0	3.3	0.0	52.9	46.1 (45.9)
β-D-Gal-1C (**XXIIb**)	*aa*	1.2	0.0	1.7	0.3	0.2	0.0	2.2	0.0	54.8	48.2 (45.9)

[a] In parentheses are given the experimental coupling constants from review [3].

[b] Lone electron pair.

Table 4. Contributions (Hz) of LMOs to the $^{13}C–^{13}C$ coupling constants of α- and β-D-mannose C1, calculated by the CLOPPA INDO method

LMO	α-D-Man-C1 (**XVa**)	β-D-Man-C1 (**XVIa**)
C^1-C^2	53.4	51.2
C^1-H	1.8	–0.3
C^1-O^1	0.3	0.1
C^1-O^5	0.8	0.4
C^2-H	2.8	2.9
C^2-O^2	0.0	0.0
C^2-C^3	2.4	1.8
O^1-H	0.0	0.0
O^1 (LEP)	0.6	1.0
O^5-C^5	0.0	0.0
O^5 (LEP)	0.0	0.0
O^2-H	0.0	0.0
O^2 (LEP)	0.0	0.0
C^3-H	0.0	0.0
C^3-C^4	0.0	0.0
C^3-O^3	0.0	0.0
Total[a]	61.5 (46.7)	56.1 (42.7)

[a] In parentheses, the experimental values from [14] are given.

Taking into account published data on the effect of the oxygen lone electron pairs on the coupling constant $^1J_{CC}$ in alcohols [18] and ethers [19], we believed that just these and the corresponding O–H bonds will determine the difference in $^1J_{CC}$. Nevertheless, we made an attempt to analyze contributions of molecular fragments (chemical bonds and lone electron pairs), which could explain the observed stereochemical behavior of the coupling constants $^1J_{1,2}$ for different pyranose anomers and conformers.

A clear relation is seen for the $^1J_{1,2}$ values for each particular monosaccharide (Table 3). In all cases, the difference in $^1J_{1,2}$ results from the contributions of C^1-C^2 and C^1-H LMOs, i.e., of those involving the anomeric carbon atom. For example, $^1J_{1,2}$ for α-D-lyxose C1 is on the average greater by 3 Hz than $^1J_{1,2}$ for β-D-lyxose C1. This difference originates from (1) greater contribution (by ~2 Hz) of the C^1-C^2 LMO for the α-anomer and (2) greater contribution (by ~1.5 Hz) of the C^1-H LMO for the same anomer. In all other cases (Table 3), the contributions of the C^1-C^2 and C^1-H LMOs are the main factors responsible for the observed differences in $^1J_{1,2}$ between the anomers and conformers. The contributions of lone electron pairs on the oxygen atoms at C^1 and C^2 as a rule do not exceed 0.5 Hz while the differences in the $^1J_{1,2}$ values are 2–3 Hz.

Table 4 gives more detailed data on LMO contributions to the coupling constants $^1J_{1,2}$ for the α- and β-anomers of mannose (C1 conformer), for which 13 bonds and 6 lone electron pairs on three oxygen atoms were taken into account. The contributions of remote bonds (which include neither C^1 nor C^2) are insignificant, and the experimental difference between $^1J_{1,2}$ for the α- and β-anomers of mannose ($\Delta^1J_{1,2} \approx$ 4 Hz) can be explained primarily by the different contributions of C^1-C^2 ($\Delta^1J_{1,2} \approx 2$ Hz) and C^1-H LMOs ($\Delta^1J_{1,2} \approx 2$ Hz) and to a lesser extent by those of C^1-O^5 ($\Delta^1J_{1,2} \approx 0.4$ Hz) and C^1-O^1 LMOs ($\Delta^1J_{1,2} \approx 0.2$ Hz). The contributions of lone electron pairs on the anomeric oxygen atom are 0.6 and 1.0 Hz for the α-anomer and β-anomer, respectively; i.e., they "act" in the opposite direction. The contribution of the O^2 LEP is negligible.

Summarizing the data in Tables 1–3, it should be noted that the differences in $^1J_{1,2}$ for different anomers and conformers are quantitatively reproduced by the SCPT INDO calculations and that (according to the results of analysis of LMO contributions in terms of the CLOPPA approach) these differences originate mainly from the C^1-C^2 and C^1-H LMOs while the contributions of all other bonds and lone electron pairs are insignificant.

Thus our calculations show that the coupling constant between the C^1 and C^2 atoms in pyranoses is very sensitive to orientation of the anomeric hydroxy group and conformation of the pyranose ring. We were the first to reveal general relations holding in the stereochemical behavior of the $C^1–C^2$ coupling constants of pento- and hexopyranoses, which can be used for unambiguous assignment of configuration of the anomeric center and conformational analysis of carbohydrates and products of their metabolism possessing a pyranose fragment.

EXPERIMENTAL

Quantum-chemical calculations were performed with the use of SCPTINDO [13], CLOPPA [16], MOPAC [20], GAMESS [21], and DALTON [22] software packages under Linux Red Hat 7.1 (Kernel 2.4.2-2). In the SCPT INDO calculations of $^{13}C–^{13}C$ coupling constants, the following parameters were taken for carbon atoms: *s*-electron density $s^2_{C(0)}$ = 3.2328 and dimensions of 2*p* orbitals $\langle r^{-3}\rangle$ = 2.8256.

This study was financially supported by the Russian Foundation for Basic Research (project no. 98-03-32882). The authors are grateful to G.E. Sal'nikov (Novosibirsk Institute of Organic Chemistry, Siberian

Division, Russian Academy of Sciences) for kindly providing the latest versions of quantum-chemical programs and to Yu.V. Gatilov (Novosibirsk Institute of Organic Chemistry, Siberian Division, Russian Academy of Sciences) for his help in interpretation of X-ray diffraction data under financial support by the Russian Foundation for Basic Research of the license for using Cambridge Crystal Structure Database (project no. 99-07-90133).

REFERENCES

1. Serianni, A.S., *Bioorganic Chemistry: Carbohydrates*, Hecht, S.M., Ed., Oxford: Oxford Univ., 1999, p. 244; Serianni, A.S., *Stable Isotope Applications in Biomolecular Structure and Mechanisms*, Trewhella, J., Cross, T.A., and Unkefer, C.J., Eds., Los Alamos: Los Alamos National Laboratories, 1994, p. 209.
2. Serianni, A.S., *^{13}C Nuclear Magnetic Resonance Spectra of the Monosaccharides: Natural and Stable Isotopically Enriched Compounds*, New York: Omicron Biochemicals, 1986; Finley, J.W., Schmidt, S.J., and Serianni, A.S., *NMR Applications in Biopolymers*, New York: Plenum, 1990; Serianni, A.S., *Glycoconjugates: Composition, Structure, and Function*, Allen, H.J. and Kisailus, E.C., Eds., New York: Marcel Dekker, 1992, p. 71; Serianni, A.S., *NMR of Biological Macromolecules*, NATO ASI Series H: Cell Biology, 1994, vol. 87, p. 293.
3. Krivdin, L.B. and Kalabin, G.A., *Prog. NMR Spectrosc.*, 1989, vol. 21, pp. 293–448.
4. Marshall, J.L., *Carbon–Carbon and Carbon–Proton NMR Couplings: Applications to Organic Stereochemistry and Conformational Analysis*, Marchand, A.P., Ed., Deerfield Beach: Chemie, 1983; Krivdin L.B. and Zinchenko, S.V., *Curr. Org. Chem.*, 1998, vol. 2, p. 173; Krivdin, L.B. and Della, E.W., *Prog. NMR Spectrosc.*, 1991, vol. 23, pp. 301–610.
5. Wu, J., Bondo, P.B., Vuorinen, T., and Serianni, A.S., *J. Am. Chem. Soc.*, 1992, vol. 114, p. 3499.
6. King-Morris, M.J. and Serianni, A.S., *J. Am. Chem. Soc.*, 1987, vol. 109, p. 3501.
7. Cloran, F., Carmichael, I., and Serianni, A.S., *J. Am. Chem. Soc.*, 2001, vol. 123, p. 4781.
8. Becke, A.D., *J. Chem. Phys.*, 1993, vol. 98, p. 5648.
9. Lee, C., Yang, W., and Parr, R.G., *Phys. Rev. B*, 1988, vol. 37, p. 785.
10. Hariharan, P.C. and Pople, J.A., *Theor. Chim. Acta*, 1973, vol. 28, p. 213.
11. Dunning, T.H., Jr., *J. Chem. Phys.*, 1989, vol. 90, p. 1007.
12. Snyder, J.R. and Serianni, A.S., *J. Org. Chem.*, 1986, vol. 51, p. 2694.
13. Blizzard, A.C. and Santry, D.P., *J. Chem. Phys.*, 1971, vol. 55, p. 950; Blizzard, A.C. and Santry, D.P., *J. Chem. Phys.*, 1973, vol. 58, p. 4714.
14. Ramsey, N.F., *Phys. Rev.*, 1953, vol. 91, p. 303.
15. Cloran, F., Carmichael, I., and Serianni, A.S., *J. Am. Chem. Soc.*, 2000, vol. 122, p. 396.
16. Diz, A.C., Ruiz de Azua, M.C., Giribet, C.G., and Contreras, R.H., *Int. J. Quantum Chem.*, 1990, vol. 37, p. 663; Contreras, R.H., Giribet, C.G., Ruiz de Azua, M.C., Cavasotto, C.N., Aucar, G.A., and Krivdin, L.B., *J. Mol. Struct. (Theochem)*, 1990, vol. 210, p. 175.
17. Engelmann, A.R., Natiello, M.A., Scuseria, G.E., and Contreras, R.H., *Comput. Phys. Commun.*, 1986, vol. 39, p. 409; Engelmann, A.R. and Contreras, R.H., *Int. J. Quantum Chem.*, 1983, vol. 23, p. 1033.
18. Zinchenko, S.V., Krivdin, L.B., and Kalabin, G.A., *Zh. Org. Khim.*, 1990, vol. 26, p. 2474.
19. Glushko, G.N. and Krivdin, L.B., *Russ. J. Org. Chem.*, 1996, vol. 32, p. 1286; Shcherbakov, V.V., Krivdin, L.B., Glukhikh, N.G., and Kalabin, G.A., *Zh. Org. Khim.*, 1987, vol. 23, p. 1792.
20. Coolidge, M.B. and Stewart, J.J.P., *QCPE. Program 455 (Release 6.0)*, 1990.
21. Schmidt, M.W., Baldridge, K.K., Boatz, J.A., Elbert, S.T., Gordon, M.S., Jensen, J.H., Koseki, S., Matsunaga, N., Nguyen, K.A., Su, S.J., Windus, T.L., Dupuis, M., and Montgomery, J.A., *J. Comput. Chem.*, 1993, vol. 14, p. 1347.
22. Helgaker, T., Jensen, H.J.A., Joergensen, P., Olsen, J., Ruud, K., Aagren, H., Andersen, T., Bak, K.L., Bakken, V., Christiansen, O., Dahle, P., Dalskov, E.K., Enevoldsen, T., Fernandez, B., Heiberg, H., Hettema, H., Jonsson, D., Kirpekar, S., Kobayashi, R., Koch, H., Mikkelsen, K.V., Norman, P., Packer, M.J., Saue, T., Sauer, S.P.A., Taylor, P.R., and Vahtras, O., *DALTON: An Electronic Structure Program (Release 1.1)*, 2000.